Talanta 80 (2010) 1719–1724

Contents lists available at ScienceDirect

Talanta

journal homepage: www.elsevier.com/locate/talanta

Polymerized ionic liquid-wrapped carbon nanotubes: The promising composites for direct electrochemistry and biosensing of redox protein

Chunhui Xiao, Xiaochen Chu, Bohua Wu, Haili Pang, Xiaohua Zhang, Jinhua Chen*

State Key Laboratory of Chemo/Biosensing and Chemometrics, College of Chemistry and Chemical Engineering, Hunan University, Lushan Road, Changsha 410082, PR China

ARTICLE INFO

Article history:
Received 16 July 2009
Received in revised form
28 September 2009
Accepted 7 October 2009
Available online 14 October 2009

Keywords:
Polymerized ionic liquid
Carbon nanotubes
Glucose oxidase
Direct electrochemistry
Biosensing

ABSTRACT

Polymerized ionic liquid-wrapped carbon nanotubes (PIL-CNTs) were firstly designed for direct electrochemistry and biosensing of redox proteins. The CNTs were coated successfully with polymerized ionic liquid (PIL) layer, as verified by transmission electron microscopy (TEM), thermogravimetric analysis (TGA) and Fourier transform infrared (FT-IR) spectroscopy. The PIL-CNTs were dispersed better in water and showed superior electrocatalysis toward O_2 and H_2O_2 comparing to pristine CNTs and the mixture of IL monomer and CNTs. With glucose oxidase (GOD) as a protein model, the direct electrochemistry of the redox protein was investigated on the PIL-CNTs modified glassy carbon (GC) electrode and excellent direct electrochemical performance of GOD molecules was observed. The proposed biosensor (GOD/PIL-CNTs/GC electrode) displayed good analytical performance for glucose with linear response up to 6 mM, response sensitivity of 0.853 $\mu A\,mM^{-1}$, good stability and selectivity.

1. Introduction

The design of new biocompatible materials with good conductivity [1], large surface area [2], and good biocompatibility [3] for biosensors has been paid considerate attention over the last decade. Several classes of materials have been investigated including carbon [4–6], polymer [7,8], silicate [9], and metal nanoparticles [10]. Among these materials, carbon nanotubes (CNTs) are leading the development of the biosensor materials because of their outstanding physical and electronic properties (such as high conductivity, specific surface area and electrocatalytic activity) [11,12]. CNTs modified electrodes have been illustrated to improve electrochemical behavior of important biochemical matters such as hydrogen peroxide [13], NADH [14], catecholamine [15], dopamine, uric acid [16], 3,4-dihydroxyphenylacetic acid [17], hydrazine [18], and nucleic acid [19]. On the other hand, many redox proteins such as hemoglobin [20], myoglobin [21], horseradish peroxide [22], cytochrome c [23], and GOD [24,25] showed direct electron transfer in a series of CNTs modified electrodes.

On the other hand, room temperature ionic liquids (ILs), are composed of two asymmetrical ions with opposite charges that only loosely fit together with low melting point (<100 °C), high ionic conductivity and a wide electrochemical window. Due to the excellent physicochemical properties, ionic liquids have been extensively used as the modifiers for the CNT-based electrode to fabricate the biosensors with fast electron transfer rate and good enzyme stability [26–29]. Although the general method of physically mixing into composite matrix to immobilize ionic liquid units on the CNT-based electrode is facilitated, the quantity of IL unit binding on the surface of CNTs is limited and IL components leak easily from the electrode due to their wide solubility in the solutions, especially during the electrochemical measurements. Strategies in which ionic liquid monomer is directly polymerized on the surface of CNTs to form stable ionic liquid functionalized composites offer a solution to this problem. Recently, our group developed an approach to obtain high dispersion and narrow size distribution of metal nanoparticles on the surface of CNTs functionalized by polymerized ionic liquid (PIL) and the metallic nanoparticles/PIL-CNTs nanohybrids showed excellent electrocatalytic properties toward methanol oxidation [30]. However, according to our best knowledge, no works applied polymerized ionic liquid-wrapped carbon nanotubes (PIL-CNTs) to construct biosensors.

In this paper, with GOD as a protein model, we have developed a new biosensor based on the PIL-CNTs for the first time, which combined the excellent physicochemical properties of CNTs with the good biocompatibility and unique ionic properties of ILs. The immobilized GOD on the PIL-CNTs modified electrode shows excellent direct electrochemical response. This new bionanocomposite may offer an efficient strategy and a promising platform for the further study of direct electron transfer of the redox proteins and the development of biosensors.

* Corresponding author. Tel.: +86 731 8821818; fax: +86 731 8821818.
E-mail addresses: chenjinhua@hnu.cn, chenjh001@hotmail.com (J. Chen).

0039-9140/$ – see front matter © 2009 Elsevier B.V. All rights reserved.
doi:10.1016/j.talanta.2009.10.012

2. Experimental

2.1. Reagents and apparatus

Multi-walled carbon nanotubes (CNTs, >95%, diameter 20–60 nm, length 5–15 μm) prepared by chemical vapor deposition (CVD) were purchased from Shenzhen Nanotech Port Ltd., and used without any purification. 1-Vinylimidazole was purchased from Alfa Aesar. Glucose oxidase (E.C. 1.1.3.4, Type X-S, 136100 U/G from *Aspergillus niger*), 5 wt.% Nafion 117 solution was purchased from Sigma–Aldrich (USA). Glucose stock solution was stored overnight at room temperature before use. All other chemicals were of analytical grade. Aqueous solutions used throughout were prepared with double-distilled water obtained from a Millipore system (>18 MΩ cm).

Micrographs of transmission electron microscopy (TEM) were obtained on a JEOL 3010 transmission electron microscope operating at 200 kV. The characterization of PIL-CNTs analyzed by the thermogravimetric analysis (TGA) was measured by Luxx STA 409 PC with 10 °C/min heating rate in the nitrogen flow and the FT-IR spectroscopy was carried on Nicolet 6700. All electrochemical measurements were performed on a IM6ex Electrochemical Workstation (Zahner-elektrik Gmbh & Co. KG, Germany) with a conventional three-electrode cell. A platinum wire was used as the counter electrode and a saturated calomel electrode (SCE) as the reference electrode. Except the specific statement, the electrochemical measurements were carried out in a phosphate buffer solution (PBS, 0.1 M, pH 7.0) at room temperature (25 ± 2 °C). All the potentials in this paper were referred to SCE.

2.2. Preparation of the PIL-CNTs

1-Vinyl-3-ethyl imidazolium bromide ([VEIM]Br) was synthesized according to the literature [31]. In brief, the mixture of 6.54 g bromoethane and 5.00 g 1-vinylimidazole was refluxed for 3 h at 70 °C under vigorous stirring. Then the excess bromoethane was removed on a Rotavapor for 2 h at 60 °C to obtain ILs. The PIL-CNTs were fabricated by the thermal initiation free radical polymerization of IL monomer ([VEIM]Br) to form ionic liquid polymer (PIL) on the CNT surface: a mixture of [VEIM]Br (1.56 g) and CNT powder (200 mg) was mixed and ground in an agate mortar for 30 min, subsequently mixed with 2,2′-azobisisobutyronitrile (AIBN 76 mg) as an initiator. The mixture was then placed in a flask and heated at 80 °C under nitrogen protection for 12 h. The formed black polymeric gel was then washed by ethanol to remove AIBN and unreacted monomer of [VEIM]Br. Finally the polymeric bucky gel was dried in vacuum at 60 °C for 12 h after centrifugation.

2.3. Preparation of PIL-CNTs modified electrode

Prior to use, glassy carbon electrodes (GC, 3 mm in diameter) were carefully polished to a mirror-like plane with 0.5- and 0.05-μm alumina slurries successively, followed by rinsing thoroughly with double-distilled water and dried in nitrogen atmosphere.

The PIL-CNTs modified electrode was prepared by casting 8 μL of uniform PIL-CNTs suspension (1.5 mg/mL) on the GC surface and dried under an infrared lamp. In control experiments, the CNTs (or ILs-CNTs) modified GC electrode was prepared by casting pristine CNTs (or ILs-CNTs) on the GC electrode according to the above procedure. Pristine CNTs was dispersed in DMF for better solubility and ILs-CNTs sample was prepared by dispersing ILs monomer and pristine CNTs (w/w = 35:65) in water.

For fabricating GOD biosensor, a 5 μL of GOD solution (10 mg mL^{-1} GOD in PBS, pH 7.0) was dropped on the PIL-CNTs modified GC electrode and dried at less than 4 °C, the obtained GOD/PIL-CNTs modified electrode was then washed carefully with double-distilled water and dried, followed by coating 1.5 μL of Nafion ethanol solution (1 wt.%) onto the electrode surface to avoid the leak of the GOD. The Nafion/GOD/PIL-CNTs electrode was washed thoroughly with double-distilled water. For comparison, CNTs modified electrode was also used to immobilize GOD via same procedure.

3. Results and discussion

3.1. Characterization of the PIL-CNTs nanocomposite

During the polymerization process, oligomeric 1-vinyl-3-ethyl imidazolium ion-base ionic liquid radicals, because of the strong π–π stacking interaction between the imidazolium ion moieties and CNTs, would attach to the surface of nanotubes, leading to the formation of PIL layer on the CNT surface [32,33]. Fig. 1A and B shows the TEM images of the PIL-CNTs. It can be observed that a PIL layer with the thickness of 7–8 nm presents on the outside wall of CNTs. Noteworthy is that the PIL layer is distributed uniformly along the whole tubes, which would create a uniform distribution of ionic species with positive charge that prevents aggregation of CNTs and induces stable nanotube suspensions in water.

The modification of CNTs by PIL has also been characterized by TGA and FT-IR. Fig. 1C shows the TGA spectra of the CNTs and PIL-CNTs. Comparing to the CNTs sample, the PIL-CNTs sample shows a significant weight loss in the range of 500–700 K, which confirms the PIL functionalization of CNTs. A ratio of PIL:CNTs in the as-prepared PIL-CNTs sample is also obtained to be about 35:65 (w/w). In addition, both of the PIL-CNTs and CNTs have been characterized by FT-IR spectroscopy (Fig. 1D), which shows a C=N stretch at 1500–1600 cm^{-1}. The peak of 1200 and 1258 cm^{-1} is strengthened by the modification of PIL, which may be due to increased C–N functional group from PIL.

3.2. Electrocatalysis of O_2 and H_2O_2 at the PIL-CNTs modified GC electrode

Fig. 2A shows the cyclic voltammograms (CVs) of bare GC, CNTs/GC, ILs-CNTs/GC and PIL-CNTs/GC electrodes in 0.1 M PBS (pH = 7.0) saturated with O_2 (or degassed with N_2). For the CNTs/GC, ILs-CNTs/GC and PIL-CNTs/GC electrodes, an obvious reduction wave of O_2 starts at about −0.16 V. However, for the bare GC electrode, the onset potential for O_2 reduction is about −0.32 V. It is further noted that the reduction current of O_2 on the PIL-CNTs/GC is obviously higher than that on the ILs-CNTs/GC, CNTs/GC, and bare GC electrodes and the following order can be obtained: PIL-CNTs/GC ≫ CNTs/GC ≅ ILs-CNTs/GC ≫ bare GC. This implies that the PIL-CNTs/GC electrode has the highest electrocatalytic activity for O_2 reduction, which should be beneficial to the third generation enzyme biosensors. In addition, H_2O_2 is an intermediate in most oxidase-based enzymatic reaction. Therefore, the electrocatalytic properties of the PIL-CNTs composite for the redox of H_2O_2 have also been investigated. Fig. 2B shows the background-subtracted CVs of the bare GC, CNTs/GC, ILs-CNTs/GC and PIL-CNTs/GC electrodes in 0.1 M PBS with 5 mM H_2O_2. The following order of the oxidation (or reduction) current of H_2O_2 at different electrodes can be observed: PIL-CNTs/GC ≫ ILs-CNTs/GC ≅ CNTs/GC ≫ bare GC. It is also noted that the PIL-CNTs/GC electrode has the highest electrocatalytic activity for H_2O_2 oxidation and reduction. The superior electrocatalytic activity toward O_2 reduction and H_2O_2 oxidation (reduction) of the PIL-CNTs/GC electrode might originate from the synergistic effect between the CNTs and PIL. Such excellent electrocatalytic activities for O_2 reduction and H_2O_2 oxidation (reduction) should lead to good properties of the PIL-CNT-based biosensors.

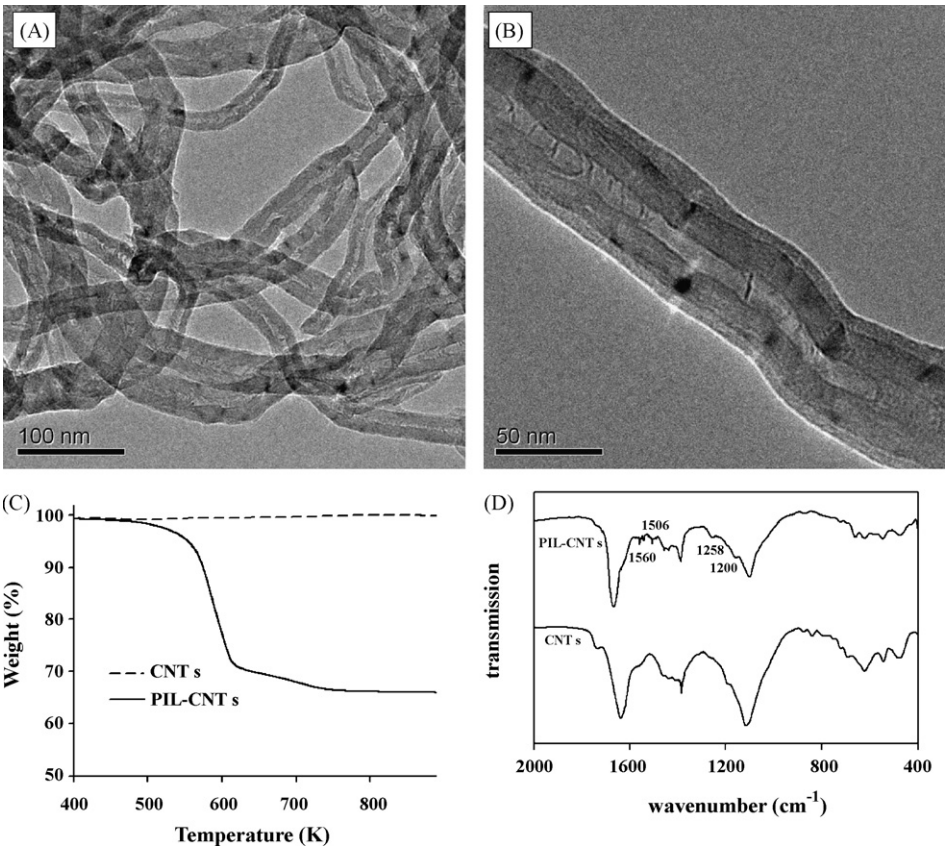

Fig. 1. TEM images of the PIL-CNTs at different magnifications (A and B) and TGA (C), FT-IR (D) spectra of PIL-CNTs and CNTs.

3.3. *Direct electrochemistry of the Nafion/GOD/PIL-CNTs/GC electrode*

In order to explore the application of PIL-CNTs composite in biosensors, GOD was selected as the model and the direct electrochemistry of the immobilized GOD on the PIL-CNTs/GC electrode has been investigated. Fig. 3 shows the cyclic voltammograms of the different electrodes in 0.1 M nitrogen-saturated PBS (pH 7.0) at 50 mV s^{-1}. A pair of well-defined and nearly symmetric redox peaks is observed on both of CNTs (solid) and PIL-CNTs modified electrodes (dashed) with immobilized GOD, while the related electrodes without GOD do not show such redox waves in the control experiments. This indicates that the redox waves are ascribed only to GOD redox. These features are the characteristics of the nearly reversible electron transfer process of the redox active centre (flavin adenine dinucleotide, FAD) in GOD biomolecules, suggesting that the direct electron transfer of GOD can be achieved on both CNTs and PIL-CNTs modified electrodes. From the integration of the reduction peak of GOD, the surface coverage of GOD on the Nafion/GOD/CNTs/GC and Nafion/GOD/PIL-CNTs/GC electrodes can be calculated to be 1.84 and 4.30×10^{-9} mol cm^{-2}, respectively. It is noted that GOD immobilized on the PIL-CNTs/GC electrode is much larger than that on the CNTs/GC electrode, demonstrating that the PIL-CNTs modified electrode is more beneficial to the immobilization of GOD than the CNTs modified electrode. All those may ascribe to the uniform distribution of ionic species with positive

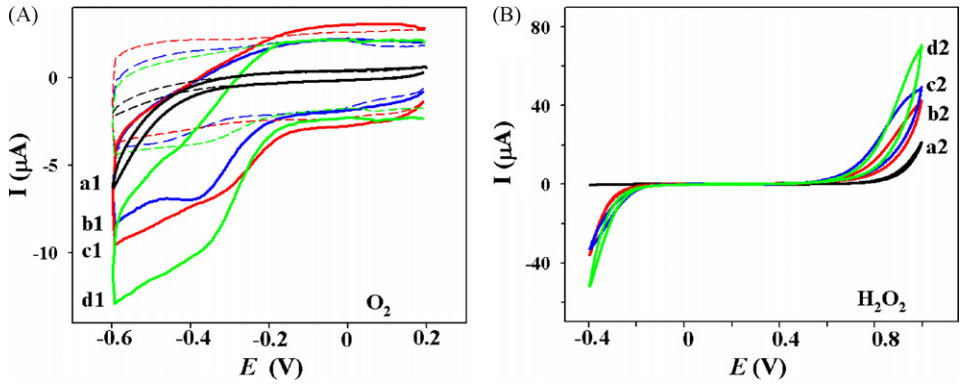

Fig. 2. (A) Cyclic voltammograms of the GC (black), CNTs/GC (red), ILs-CNTs/GC (blue) and PILs-CNTs/GC (green) electrodes in 0.1 M PBS solution saturated with O_2 (solid) or degassed with pure N_2 (dotted). Scan rate: 50 mV s^{-1}. (B) Background-subtracted CVs for 5 mM H_2O_2 at GC (black), CNTs/GC (red), ILs-CNTs/GC (blue) and PILs-CNTs/GC (green) electrodes in 0.1 M PBS solution. Scan rate: 50 mV s^{-1}. (For interpretation of the references to color in this figure legend, the reader is referred to the web version of the article.)

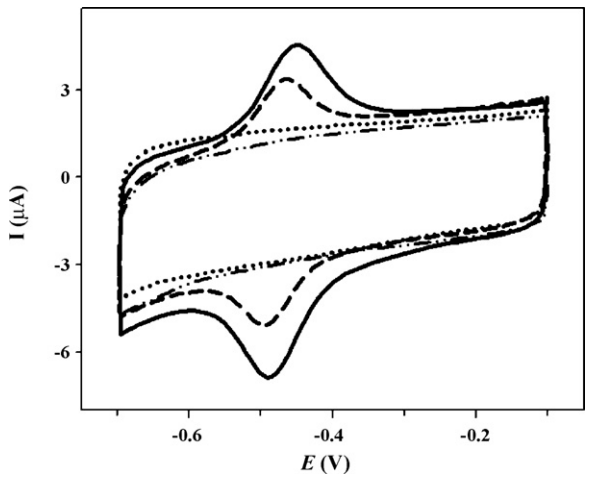

Fig. 3. Cyclic voltammograms of the Nafion/GOD/PIL-CNTs (solid), PIL-CNTs (dotted), Nafion/GOD/CNTs (dashed), CNTs (dashed-dotted) modified GCE in 0.1 M deoxygenated PBS (pH 7.0) at the scan rate of 50 mV s^{-1}.

charge present on the PIL-CNTs, resulting in more GOD molecules to be immobilized on the PIL-CNTs through electrostatic interaction between GOD (net negatively charged in the pH 7.0 PBS solution) and PIL-CNTs (positively charged). The more GOD molecules immobilized on the electrode imply that the Nafion/GOD/PIL-CNTs/GC electrode should have better analytical performance. On the other hand, for the Nafion/GOD/PIL-CNTs/GC electrode, the formal potential (E^0) was calculated by averaging the cathodic and anodic peak potentials and is ca. −0.471 V, which is close to the values reported previously [34,35]. The related anodic peak potential ($E_{p,a}$) and cathodic peak potential ($E_{p,c}$) are −0.455 and −0.487 V, respectively and the peak-to-peak potential separation is about 32 mV. The small peak-to-peak potential separation value indicates that GOD immobilized on the PIL-CNTs/GC electrode has a fast electron transfer rate, due to the strong interaction of GOD with the PIL-CNTs and the high conductivity of the PIL-CNTs [35].

The effect of the scan rate on the cyclic voltammetric response of the Nafion/GOD/PIL-CNTs/GC is shown in Fig. 4A and B. The anodic and cathodic peak currents increase linearly with the increase of the scan rate from 25 to 225 mV s^{-1}, indicating that the GOD immobilized on the PIL-CNTs/GC electrode demonstrates a surface-controlled process, not a diffusion-controlled process. It is well known that the direct electrochemistry of GOD is a two-electron coupled with two-proton reaction, which undergoes a redox reaction as follows [36]:

$$\text{GOD-FAD} + 2e^- + 2H^+ \leftrightarrow \text{GOD-FADH}_2 \quad (1)$$

Based on Eq. (1), the direct electron transfer process of GOD will be affected by the solution pH value. Fig. 4C shows the cyclic voltammograms of the Nafion/GOD/PIL-CNTs/GC electrode in the PBS with different pH values. From Fig. 4C, stable and well-defined cyclic voltammograms can be observed in the pH range of 5.0–8.0. The increase of the solution pH value causes a negative shift of both cathodic and anodic peak potentials. Fig. 4D shows the effect of the solution pH value on the formal potential (E^0) of the Nafion/GOD/PIL-CNTs/GC electrode. It can be seen that the formal potential depends linearly on the pH value in the range of 5.0–8.0 with a slop of −52.7 mV/pH (r = 0.9971), which is close to the theoretical value of −58.6 mV/pH according to the reaction shown in Eq. (1).

3.4. Biosensing application of the Nafion/GOD/PIL-CNTs modified GC electrode

On the basis of the high electrocatalytic activity of the PIL-CNTs nanocomposite toward O_2 reduction and good direct electrochemical behavior of GOD on the PIL-CNTs/GC electrode, a third

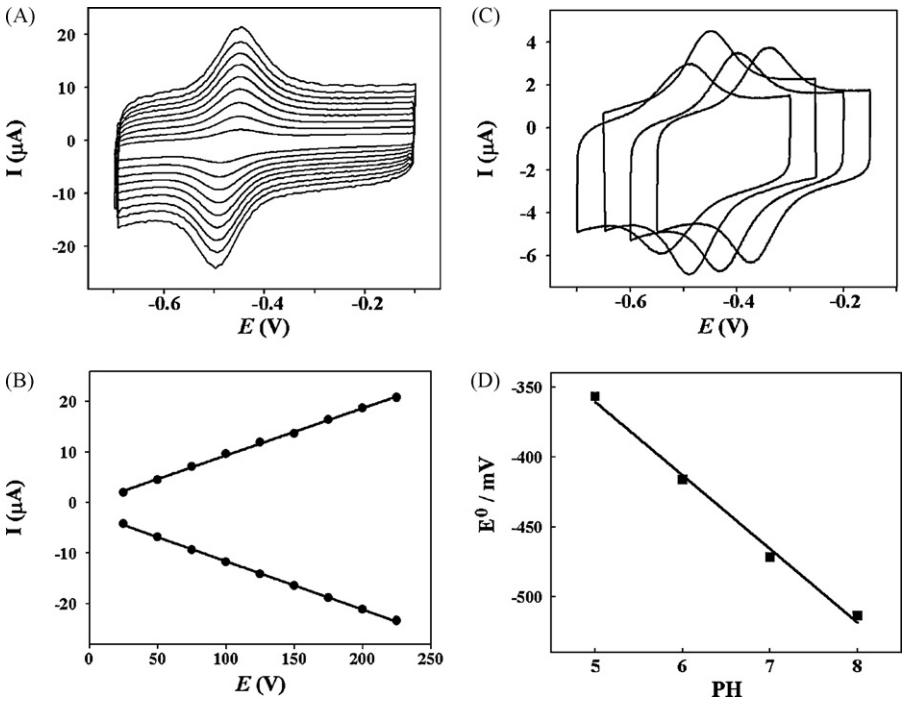

Fig. 4. (A) Cyclic voltammograms of the Nafion/GOD/PIL-CNTs modified GC electrode in 0.1 M deoxygenated PBS (pH 7.0) at scan rates of 25, 50, 75, 100, 125, 150, 175, 200, 225 mV s^{-1} (from inner to outer). (B) The dependence of the anodic and cathodic peak currents versus the scan rate. (C) Cyclic voltammograms of the Nafion/GOD/PIL-CNTs modified GC electrode in 0.1 M deoxygenated PBS with pH values of 5.0, 6.0, 7.0, and 8.0. Scan rate, 50 mV s^{-1}. (D) The dependence of the formal potential of the Nafion/GOD/PIL-CNTs modified GC electrode on the pH value.

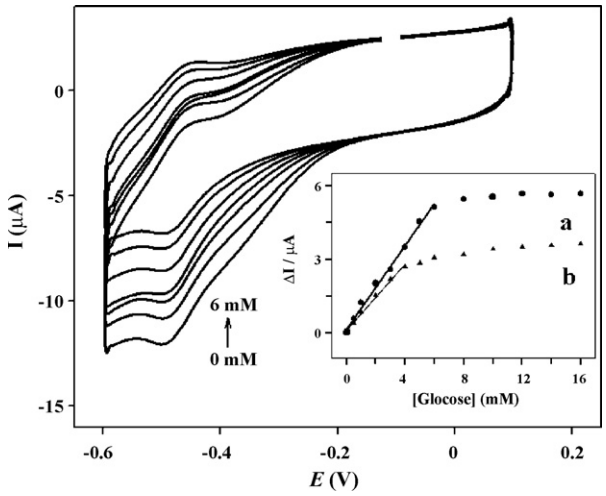

Fig. 5. Cyclic voltammograms of the Nafion/GOD/PIL-CNTs modified GC electrode in 0.1 M air-saturated PBS (pH 7.0) containing 0, 1, 2, 3, 4, 5 and 6 mM of glucose (from bottom to top) at the scan rate of 50 mV s^{-1}. The insert plot shows the dependence of the decreased reduction peak current of the Nafion/GOD/PIL-CNTs modified GC electrode (a) and Nafion/GOD/CNTs modified GC electrode (b) on the concentration of glucose in 0.1 M air-saturated PBS (pH 7.0).

generation glucose biosensor was developed further. Fig. 5 shows cyclic voltammograms of the Nafion/GOD/PIL-CNTs/GC electrode in 0.1 M air-saturated PBS (pH 7.0) with different concentrations of glucose (0.05–6 mM). The reduction current becomes smaller and smaller with the increase of the glucose concentration because of the consumption of dissolved oxygen. The insert plot in Fig. 5 shows the relationship between the decrease of the reduction peak current and the glucose concentration at the Nafion/GOD/PIL-CNTs/GC (a) and Nafion/GOD/CNTs/GC (b) electrodes. The linear response ranges for the Nafion/GOD/PIL-CNTs/GC and Nafion/GOD/CNTs/GC electrodes are 0.05–6 mM (R = 0.9946) and 0.05–4 mM (R = 0.9955), respectively. It is noted that the Nafion/GOD/PIL-CNTs/GC electrode has wider linear range than Nafion/GOD/CNTs/GC electrode. Furthermore, the sensitivity of the Nafion/GOD/PIL-CNTs/GC electrode is calculated to be 0.853 μA mM^{-1}, which is higher than that of Nafion/GOD/CNTs/GC electrode (0.676 μA mM^{-1}) and other third generation glucose biosensors reported in literatures [37–39].

To evaluate the stability of the electrode, the cyclic voltammetry measurements were carried out continuously in a 0.1 M PBS (pH 7.0). The decrease in the peak currents can be observed on both Nafion/GOD/PIL-CNTs and Nafion/GOD/CNTs electrodes. However, after 40 cycles, the decrease in the peak currents is less than 6% for the Nafion/GOD/PIL-CNTs/GC electrode and more than 20% for the Nafion/GOD/CNTs/GC electrode. It is noted further that more than 90% of peak current on Nafion/GOD/PIL-CNTs/GC electrode is retained even after 100 cycles successively scan in 0.1 PBS (pH 7.0). This implies that the Nafion/GOD/PIL-CNTs/GC electrode has better stability than the Nafion/GOD/CNTs/GC electrode, which may result from the additional electrostatic interaction between the positive sites on the PIL and negative charges in the GOD (FAD). Additionally, when the Nafion/GOD/PIL-CNTs/GC electrode was stored in 0.1 M PBS at 4 °C, it retains 94% of its initial current response toward glucose after intermittent use over a 2-week period, further corroborating the good stability of the biosensor and high efficiency of PIL-CNTs for retaining the activity of the enzyme.

Because of the low detection potential, the biosensor also shows good selectivity for glucose. In an air-saturated and stirred 0.1 M PBS solution (pH 7.0) containing 0.5 mM glucose, the response arising from 0.01 mM uric acid (UA) and 0.01 M ascorbic acid (AA) is negligible. The reproducibility of the glucose biosensor was also investigated by detecting the current response at −0.49 V to 2 mM glucose in the PBS for six successive times, the relative standard deviation (RSD) is 3.3%, demonstrating a good reproducibility of the biosensor.

4. Conclusion

In this work, we demonstrated the PIL-CNTs bionanocomposite for direct electrochemistry and biosensing application of redox protein. Due to the uniform distribution of ionic species layer and good stability of IL units, the PIL-CNTs show superior electrocatalytic activity for O_2 reduction and H_2O_2 oxidation (reduction) and provide a promising platform for direct electrochemistry of GOD. The immobilized GOD on the PIL-CNTs modified GC electrode shows good direct electrochemical response and biosensing performance for glucose. All these characteristics suggest that PIL-CNTs nanocomposite provides a potential material for direct electrochemistry and biosensing of redox proteins.

Acknowledgments

This work was financially supported by NSFC (20675027, 20975033) and the Program for Fu-Rong Scholar in Hunan Province, China.

References

[1] S. Sampath, O. Lev, Anal. Chem. 68 (1996) 2015–2021.
[2] Z.H. Dai, S.Q. Liu, H.X. Ju, H.Y. Chen, Biosens. Bioelectron. 19 (2004) 861–867.
[3] P. Roach, D. Farrar, C.C. Perry, J. Am. Chem. Soc. 127 (2005) 8168–8173.
[4] J.J. Gooding, R. Wibowo, J.Q. Liu, W.R. Yang, D. Losic, S. Orbons, F.J. Mearns, J.G. Shapter, D.B. Hibbert, J. Am. Chem. Soc. 125 (2003) 9006–9007.
[5] M. Hartmann, A. Vinu, Chem. Mater. 17 (2005) 829–833.
[6] A. Vinu, M. Miyahara, K.J. Ariga, Phys. Chem. B 109 (2005) 6436–6441.
[7] B.S. Lele, H. Murata, K. Matyjaszewski, A.J. Russell, Biomacromolecules 6 (2005) 3380–3387.
[8] A. Lewis, Y.Q. Tang, S. Brocchini, J.W. Choi, A. Godwin, Bioconjug. Chem. 19 (2008) 2144–2155.
[9] Y. Han, S. Lee, J. Ying, Chem. Mater. 18 (2006) 643–649.
[10] I. Lynch, K.A. Dawson, Nano Today 3 (2008) 40–47.
[11] Y.D. Zhao, W.D. Zhang, H. Chen, Q.M. Luo, Talanta 58 (2002) 529–534.
[12] J. Zhong, L. Song, J. Meng, B. Gao, W.S. Chu, H.Y. Xu, Y. Luo, J.H. Guo, A. Marcelli, S.S. Xie, Z.Y. Wu, Carbon 47 (2009) 967–973.
[13] J. Wang, M. Musameh, Y.H. Lin, J. Am. Chem. Soc. 125 (2003) 2408–2409.
[14] M. Musameh, J. Wang, A. Merkoci, Y.H. Lin, Electrochem. Commun. 4 (2002) 743–746.
[15] J. Wang, M. Li, Z. Shi, N. Li, Z. Gu, Electroanalysis 14 (2002) 225–230.
[16] Z.H. Wang, J. Liu, Q.L. Liang, Y.M. Wang, G. Luo, Analyst 127 (2002) 653–658.
[17] J.X. Wang, M.X. Li, Z.J. Shi, N.Q. Li, Z.N. Gu, Electrochim. Acta 47 (2001) 651–657.
[18] H.T. Zhao, H.X. Ju, Anal. Biochem. 350 (2006) 138–144.
[19] C.V. Nguyen, L. Delzeit, A.M. Cassell, J. Han, M. Meyyappan, Nano Lett. 2 (2002) 1079–1081.
[20] H.Y. Zhao, W. Zheng, Z.X. Meng, H.M. Zhou, X.X. Xu, Z. Lia, Y.F. Zheng, Biosens. Bioelectron. 24 (2009) 2352–2357.
[21] C.Y. Liu, J.M. Hu, Biosens. Bioelectron. 24 (2009) 2149–2154.
[22] Z.J. Cao, X.Q. Jiang, Q.J. Xie, S.Z. Yao, Biosens. Bioelectron. 24 (2008) 222–227.
[23] C.L. Xiang, Y.J. Zou, L.X. Sun, F. Xu, Electrochem. Commun. 10 (2008) 38–41.
[24] Q. Liu, X.B. Lu, J. Li, X. Yao, J.H. Li, Biosens. Bioelectron. 22 (2007) 3203–3209.
[25] P.P. Joshi, S.A. Merchant, Y.D. Wang, D.W. Schmidtke, Anal. Chem. 77 (2005) 3183–3188.
[26] Y.J. Zhang, Y.F. Shen, D.X. Han, Z.J. Wang, J.X. Song, F. Li, L. Niu, Biosens. Bioelectron. 23 (2007) 438–443.
[27] F. Jia, C.S. Shan, F.H. Li, L. Niu, Biosens. Bioelectron. 24 (2008) 945–950.
[28] R.T. Kachoosangi, M.M. Musameh, I. Abu-Yousef, J.M. Yousef, S.M. Kanan, L. Xiao, S.G. Davies, A. Russell, R.G. Compton, Anal. Chem. 81 (2009) 435–442.
[29] Y. Liu, L.J. Huang, S.J. Dong, Biosens. Bioelectron. 23 (2007) 35–41.
[30] B.H. Wu, D. Hu, Y.J. Kuang, B. Liu, X.H. Zhang, J.H. Chen, Angew. Chem. Int. Ed. 48 (2009) 4751–4754.
[31] X.D. Mu, J.Q. Meng, Z.C. Li, Y. Kou, J. Am. Chem. Soc. 127 (2005) 9694–9695.
[32] R. Marcilla, M.L. Curri, P.D. Cozzoli, M.T. Martinez, I. Loinaz, H. Grande, J.A. Pomposo, D. Mecerreyes, Small 2 (2006) 507–512.
[33] T. Fukushima, T. Aida, Chem. Eur. 13 (2007) 5048–5058.

[34] I. Tinoco, K. Kauer, J.C. Wang, Physical Chemistry—Principles and Applications in Biological Sciences, Prentice-Hall, Englewood Cliffs, NJ, 1978.
[35] S. Wu, H.X. Ju, Adv. Funct. Mater. 17 (2007) 585–592.
[36] C.Y. Deng, J.H. Chen, X.L. Chen, C.H. Xiao, L.H. Nie, S.Z. Yao, Biosens. Bioelectron. 23 (2008) 1272–1277.
[37] C.S. Shan, H.F. Yang, J.F. Song, D.X. Han, A. Ivaska, L. Niu, Anal. Chem. 81 (2009) 2378–2382.
[38] X.D. Shangguan, H.F. Zhang, J.B. Zheng, Electrochem. Commun. 10 (2008) 1140–1143.
[39] L.D. Zhu, R.L. Yang, J.G. Zhai, C.Y. Tian, Biosens. Bioelectron. 23 (2007) 528–535.